JACS
JOURNAL OF THE AMERICAN CHEMICAL SOCIETY

Article

pubs.acs.org/JACS

Higher Order π-Conjugated Polycyclic Hydrocarbons with Open-Shell Singlet Ground State: Nonazethrene versus Nonacene

Rui Huang,[†,‡] Hoa Phan,[†] Tun Seng Herng,[§] Pan Hu,[†] Wangdong Zeng,[†] Shao-qiang Dong,[†] Soumyajit Das,[†] Yongjia Shen,[‡] Jun Ding,[§] David Casanova,*[,∥] and Jishan Wu*[,†,⊥]

[†]Department of Chemistry, National University of Singapore, Science Drive 3, 117543, Singapore

[‡]Key Laboratory of Advanced Material, Department of Chemistry, East China University of Science and Technology, 130 Meilong Road, Shanghai, 200237, China

[§]Department of Materials Science and Engineering, National University of Singapore, 119260, Singapore

[∥]IKERBASQUE - Basque Foundation for Science & Donostia International Physics Center & Kimika Fakultatea, Euskal Herriko Unibertsitatea, Paseo Manuel de Lardizabal, 4, 20018 Dgonostia-San Sebastián, Euskadi, Spain

[⊥]Institute of Materials Research and Engineering, A*STAR, 2 Fusionopolis Way, Innovis #08-03, 138634, Singapore

Supporting Information

ABSTRACT: Higher order acenes (i.e., acenes longer than pentacene) and extended zethrenes (i.e., zethrenes longer than zethrene) are theoretically predicted to have an open-shell singlet ground state, and the radical character is supposed to increase with extension of molecular size. The increasing radical character makes the synthesis of long zethrenes and acenes very challenging, and so far, the longest reported zethrene and acene derivatives are octazethrene and nonacene, respectively. In addition, there is a lack of fundamental understanding of the differences between these two closely related open-shell singlet systems. In this work, we report the first synthesis of a challenging nonazethrene derivative, **HR-NZ**, and its full structural and physical characterizations including variable temperature NMR, ESR, SQUID, UV−vis−NIR absorption and electrochemical measurements. Compound **HR-NZ** has an open-shell singlet ground state with a moderate diradical character (y_0 = 0.48 based on UCAM-B3LYP calculation) and a small singlet−triplet gap (ΔE_{S-T} = −5.2 kcal/mol based on SQUID data), thus showing magnetic activity at room temperature. It also shows amphoteric redox behavior, with a small electrochemical energy gap (1.33 eV). Its electronic structure and physical properties are compared with those of Anthony's nonacene derivative **JA-NA** and other zethrene derivatives. A more general comparison between higher order acenes and extended zethrenes was also conducted on the basis of *ab initio* electronic structure calculations, and it was found that zethrenes and acenes have very different spatial localization of the unpaired electrons. As a result, a faster decrease of singlet−triplet energy gap and a faster increase of radical character with increase of the number of benzenoid rings were observed in zethrene series. Our studies reveal that spatial localization of the frontier molecular orbitals play a very important role on the nature of radical character as well as the excitation energy.

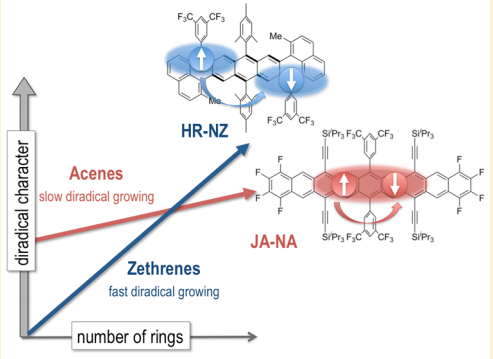

INTRODUCTION

π-Conjugated polycyclic hydrocarbons (CPHs) with an open-shell singlet ground state have recently attracted much attention in the frontier areas of physical organic chemistry, structural organic chemistry, and materials science.[1] Among various studied CPHs,[2−5] higher order acenes (longer than pentacene)[6] and extended zethrenes (longer than zethrene)[7] are two closely related systems (Figure 1a), but they behave quite differently and need more detailed examination. Acenes are linearly fused benzene oligomers, and according to Clar's sextet rule, higher order acenes will be highly reactive as only one aromatic sextet ring (the ring shaded in blue color in Figure 1a) can be drawn no matter how long the acene molecule is. This simple analysis can explain the observed high reactivity of high-order parent acenes and even their derivatives. Bendikov et al. first examined the ground-state electronic structures of higher order acenes by using broken-symmetry DFT calculations (UB3LYP) and found that for acenes longer than hexacene the open-shell singlet solution is lower than that of closed-shell singlet; thus, they should have an open-shell singlet ground state.[8] Further theoretical studies indicated that longer acenes could even show polyradical character by recovering more aromatic sextet rings in the polyradical form (Figure 1a).[9] In the past decade, various stabilizing strategies have been developed by chemists, and relatively stable acenes up to nonacene have been successfully synthesized.[10] It is worth noting that Anthony's group has reported the elegant synthesis

Received: June 15, 2016
Published: July 20, 2016

DOI: 10.1021/jacs.6b06188
J. Am. Chem. Soc. 2016, 138, 10323−10330

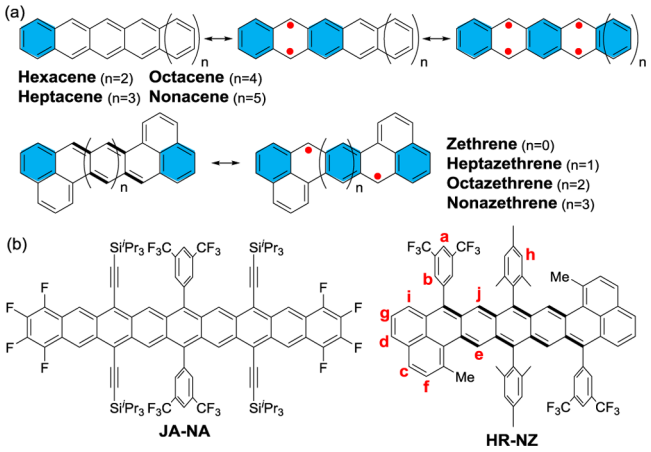

Figure 1. (a) Resonance structures of higher order acenes and extended zethrenes; (b) Chemical structures of Anthony's nonacene derivative (**JA-NA**) and our new nonazethrene derivative (**HR-NZ**).

and crystallographic structure of nonacene derivative **JA-NA** substituted by electron-withdrawing fluorine atoms and bulky triisopropylsilylethynyl and 3,5-trifluoromethylphenyl groups (Figure 1b).[10h] However, no clear conclusion was made regarding their open-shell singlet diradical character.

In parallel to the acene chemistry, our group and others have been working on a type of Z-shaped CPHs called zethrenes, which can be regarded as dibenzo-acenes.[7] The smallest member of this family is called zethrene (Zth) and the extended homologues are heptazethrene (HZ), octazethrene (OZ), nonazethrene (NZ), and so on, based on the number of the hexagon rings. Unlike acenes, extended zethrenes (from heptazethrene) have a quinoidal structure with two aromatic sextet rings in the closed-shell form and tend to become a diradical by recovering the aromaticity of the central quinodimethane moieties (Figure 1a). As a result, open-shell singlet diradical character was experimentally observed for the derivatives of heptazethrene[7d] and octazethrene.[7e] A prominent feature is the observation of thermal population from singlet to triplet state at room temperature, which results in nuclear magnetic resonance (NMR) signal broadening and paramagnetic signal in electron spin resonance (ESR) spectrum. Similar to higher order acenes, the more extended zethrenes are supposed to be extremely reactive due to the increased diradical character, but so far, there is no report on the synthesis or characterization of a stable nonazethrene derivative, the counterpart of nonacene. In this context, herein we report the first synthesis and characterization of a relatively stable nonazethrene derivative **HR-NZ**, which is kinetically stabilized by bulky mesityl and electron-deficient 3,5-trifluoromethylphenyl groups (Figure 1b). This allows us to have an experimental comparison between our nonazethrene derivative **HR-NZ** and Anthony's nonacene derivative **JA-NA**. Generally, a comparison between higher order acenes and zethrenes will give some insight into the fundamental difference between these two types of open-shell singlet CPHs.

RESULT AND DISCUSSION

Synthesis. Compound **HR-NZ** was synthesized by an intramolecular Friedel–Crafts alkylation followed by oxidative dehydrogenation approach, with compound **5** as the key intermediate (Scheme 1). The synthesis commenced with the methylation of the anthraflavic acid by using dimethyl sulfate, giving compound **1** in 90% yield. Compound **1** was then treated with excessive 2-mesitylithium and subsequent reduction by $SnCl_2$ afforded 2,6-dimethoxy-9,10-dimesitylanthracene **2** in 70% yield. Regioselective lithiation of **2** with *n*-BuLi/tetramethylethylenediamine (TMEDA) followed by quenching with dry dimethylformamide (DMF) gave the dialdehyde **3**. Compound **3** then underwent demethylation by BBr_3 and esterification by Tf_2O to afford intermediate **5**. Suzuki coupling of **5** with (2-methylnaphthalen-1-yl) boronic acid gave **6**. Then, **6** was treated with bis(trifluoromethyl) phenylmagnesium bromide to give diol **7**, which was subjected to Friedel–Crafts alkylation reaction promoted by $BF_3{\cdot}OEt_2$ and trifluoroacetic acid (TFA) to afford dihydro precursor **8**. **HR-NZ** was finally obtained as a black solid by oxidative dehydrogenation of **8** with 2,3-dichloro-5,6-dicyano-1,4-benzoquinone (DDQ) in dichloromethane (DCM) after purification by column chromatography on triethylamine-treated silica gel under argon protection. Compound **HR-NZ** was quite sensitive to air in both solid and solution state, so only freshly prepared sample was used for physical characterizations.

Magnetic Properties. Variable temperature (VT) ^{1}H NMR spectra of **HR-NZ** in THF-d_8 were recorded in a JY NMR tube under the protection of argon, and no significant decomposition was observed during the measurement (Figure 2). **HR-NZ** showed a broadened ^{1}H NMR spectrum at room temperature. Progressively sharper peaks were found as the

Scheme 1. Synthetic Route of HR-NZ[a]

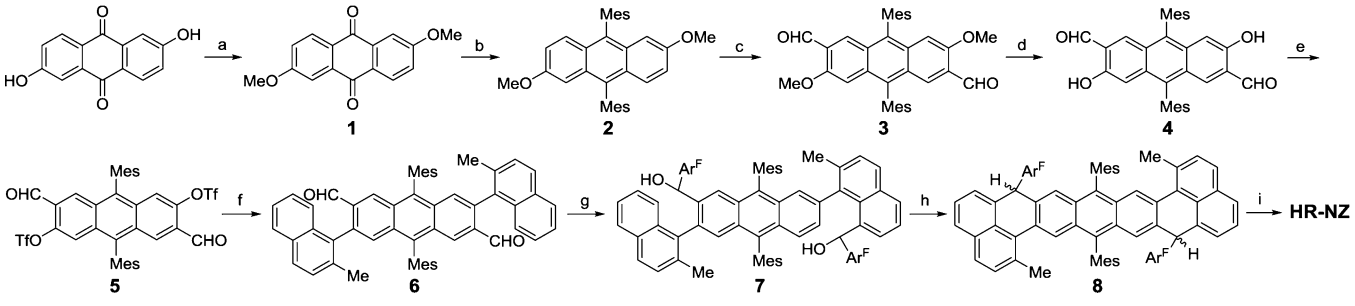

[a]Reagent and conditions: (a) dimethyl sulfate, K_2CO_3, acetone, reflux for 3 days, 90%; (b) (i) 2,4,6-trimethybromombenzene, *n*-BuLi, THF, −78 °C, overnight, (ii) $SnCl_2$, reflux, 5 h, overall yield 70%; (c) (i) *n*-BuLi, TMEDA, THF, 0 °C, 5 h; (ii) DMF, r.t., 2 h, 13%; (d) BBr_3, DCM, 0 °C, overnight, 54%; (e) $(CF_3SO_2)_2O$, pyridine, DCM, 0 °C, 2 h, 58%; (f) (2-methylnaphthalen-1-yl) boronic acid, $Pd(PPh_3)_4$, Na_2CO_3, toluene/ethanol/H_2O = 5:1:1, 95 °C, 2 days, 62%; (g) 3,5-bis(trifluoromethyl)phenylmagnesium bromide, THF, 0 °C, overnight, 90%; (h) $BF_3{\cdot}Et_2O$, TFA, DCM, 90%; (i) DDQ, DCM, under argon, 20%. Mes: mesityl; Ar^F: 3,5-bis(trifluoromethyl)phenyl.

DOI: 10.1021/jacs.6b06188
J. Am. Chem. Soc. 2016, 138, 10323–10330

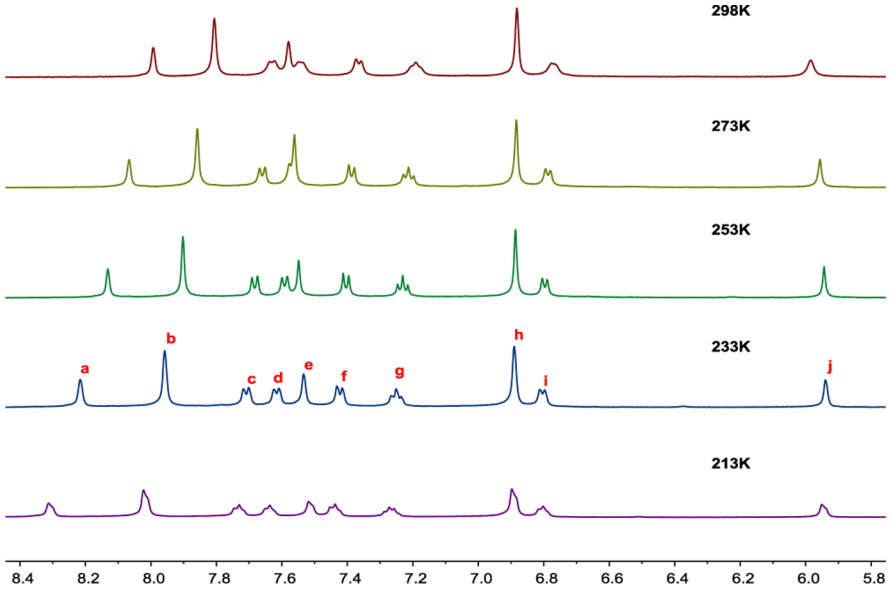

Figure 2. Variable temperature ^{1}H NMR spectra (in aromatic region) of **HR-NZ** in THF-d_8.

temperature became lower. With the help of 2D COSY measurement at 233 K (Figure S3), the NMR peaks in the aromatic region could be assigned to the proposed **HR-NZ** structure (Figure 2). This phenomenon is common for many other open-shell singlet diradicaloids, and the NMR broadening can be explained by the presence of thermally populated triplet species caused by a small singlet−triplet energy gap.

A strong, broad ESR signal with a g_e value of 2.0027 was observed for both solid and DCM solution of **HR-NZ** (Figure 3a), which is typical for largely delocalized singlet diradicaloids. The superconducting quantum interference device (SQUID) measurement was conducted on the freshly prepared powder of **HR-NZ** at the temperature range of 2−380 K. It is found that the χT product increases with increase of temperature after 250 K, correlating to a thermal population from singlet to paramagnetic triplet state (Figure 3b). The singlet−triplet energy gap (ΔE_{S-T}) was estimated to be −5.2 kcal/mol by a careful fitting of the data using the Bleaney−Bowers equation,[11] which is close to the calculated value ($\Delta E_{S-T} \approx -5.4$ kcal/mol, *vide infra*). For comparison, the freshly prepared **JA-NA** solution was reported to be ^{1}H NMR silent at room temperature, and a weak and broad ESR signal (g_e= 2.0060) was observed at both room temperature and 115 K.[10h] Upon standing, decomposition happened, resulting in new ^{1}H NMR signals for decomposed products appearing and the ESR signal eventually disappearing. There was no clear conclusion on the origin of the observed ESR signal, and a combination of VT NMR, ESR, and SQUID measurements may solve the puzzle.

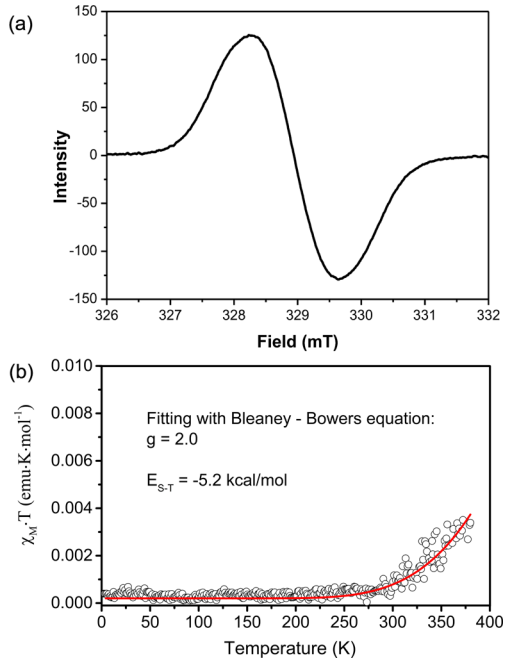

Figure 3. (a) ESR spectrum of **HR-NZ** in DCM recorded at −40 °C. (b) $\chi T-T$ plot for the solid sample of **HR-NZ** in SQUID measurements. The measured data were plotted as open circles, and the red solid curve is the best fit using Bleaney−Bowers equation with g_e = 2.00.

Optical and Electrochemical Properties. **HR-NZ** shows green color as DCM solution and its absorption spectrum shows an intense *p*-band with maximum at 672 nm ($\varepsilon = 7.96 \times 10^4$ M^{-1} cm^{-1}) (Figure 4a and Table 1). Like other open-shell singlet diradicaloids such as octazethrene derivatives, two weak shoulder absorption bands at 800 and 895 nm were observed at the low-energy absorption side, which can be correlated to the (H,H → L,L) doubly excited singlet excited state.[12,13] Solution of **HR-NZ** turned from green to brown within 1 day at both room temperature and 0 °C after removal from the glovebox, and photostability tests revealed that the half-life time of **HR-NZ** was 16 h under ambient air and light condition (Figure S5), which makes single-crystal growth unsuccessful even in a glovebox. For comparison, **JA-NA** is an olive color in toluene, showing an intense S0−S1 transition at 1014 nm and a relatively weak *p*-band at 880 nm, somewhat similar to that of **HR-NZ** except for the relative intensity of the *p*-band to the lowest energy S0−S1 absorption band, implying its open-shell diradical character. The optical energy gap (E_g^{opt}) of **JA-NA** (1.20 eV) is smaller than that of **HR-NZ** (1.33 eV). So far, stable derivatives of octacene are still not available, and the reported heptacene derivatives show a weak low-energy shoulder in addition to the major *p*-band,[10b,f] indicating their

DOI: 10.1021/jacs.6b06188
J. Am. Chem. Soc. 2016, 138, 10323−10330

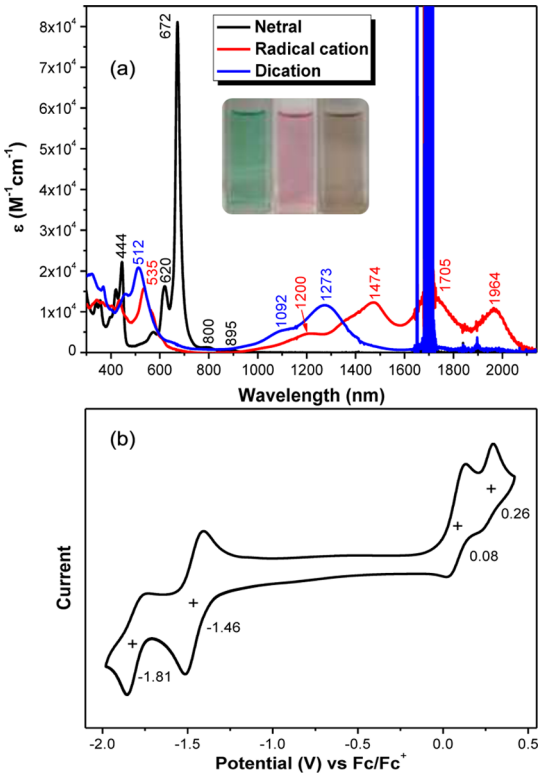

Figure 4. (a) UV−vis−NIR absorption spectra of **HR-NZ** in the neutral, radical cationic, and dicationic states in dry DCM. Inset are the photos of the solutions for the three respective states (from left to right). (b) Cyclic voltammogram of **HR-NZ** in dry DCM with 0.1 M *n*-BuNPF$_6$ as supporting electrolyte, Ag/AgCl as reference electrode, Au disk as working electrode, Pt wire as counter electrode, and scan rate at 50 mV/s.

open-shell singlet diradical character. However, clear ^{1}H NMR spectra were observed for all reported heptacene derivatives at room temperature and even at 100 °C, presumably due to the large singlet−triplet energy gaps.[10f] For all hexacene derivatives, such a fingerprint weak absorption band was not observed, which is in accordance with their small diradical character. So, hexacene and shorter acenes are better described as closed-shell CPHs.

Cyclic voltammetry (CV, Figure 4b) and differential pulse voltammetry (DPV) (Figure S4) measurements were carried out to investigate the electrochemical properties of **HR-NZ** in dry DCM solution. Two oxidation waves with half-wave potential ($E_{1/2}^{ox}$) at 0.08 and 0.26 V and two reduction waves with half-wave potential ($E_{1/2}^{red}$) at −1.46 and −1.82 V (vs Fc/Fc$^+$, Fc = ferrocene) were observed. The HOMO and LUMO energy levels were determined to be −4.73 and −3.42 eV from the onset potentials of the first oxidation and reduction wave, respectively, and the electrochemical energy gap (E_g^{EC}) was estimated to be 1.31 eV. For comparison, the HOMO and LUMO energy levels of **JA-NA** are −5.10 and −3.91 eV (Table 1); both are lower lying compared with that of **HR-NZ**, with a smaller E_g^{EC} value (1.19 eV). Compound **HR-NZ** can be chemically oxidized to stable radical cation and dication species by $NOSbF_6$ oxidant in dry DCM (Figure S6a). The monoradical cation shows intense absorption beyond 1000 nm, with maxima at 1200, 1474, 1705, and 1964 nm (HOMO → SOMO electronic transitions), together with a short wavelength absorption band at 535 nm (Figure 4a). A broad ESR signal at g_e = 2.0027 was observed (Figure S6b). This ESR signal disappeared upon further oxidation to the dication. The dication exhibits an intense absorption band in the near-infrared region with a maximum at 1273 nm and one band in the visible region with a maximum at 512 nm.

In Table 1, we also compare the photophysical and electrochemical properties of **HR-NZ** to other zethrene derivatives (Figure 5). A redshift of the absorption spectra was observed as the zethrene homologues extended. The *p*-band absorption maxima of **Zth-Mes**, **HZ-Mes**, **OZ-Mes**, and **HR-NZ** (with mesityl substitution) locate at 521, 613, 649, and 672 nm, respectively. A similar trend was also found for **Zth-APh**, **HZ-TIPS**, and **OZ-TIPS** series, but their energy gap is smaller than that of the corresponding mesityl substituted analogues due to extended electron delocalization to the

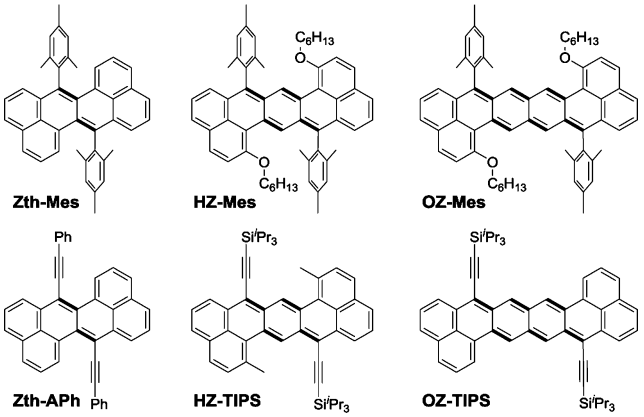

Figure 5. Structures of other reported zethrene derivatives.

Table 1. Comparison of Photophysical and Electrochemical Data between HR-NZ and JA-NA and Other Zethrene Derivatives[a]

compd	$\lambda_{(abs)}$	ε_{max}	$E_{1/2}^{ox}$	$E_{1/2}^{red}$	HOMO	LUMO	E_g^{EC}	E_g^{opt}	ΔE_{S-T}^{Exp}
Zth-Mes[7b]	521	35500						2.10	
Zth-APh[7a]	576	31600	0.29, 0.79	−1.64, −2.03	−5.05	−3.25	1.80	1.96	
HZ-Mes[7o]	613	70030	−0.27, 0.17	−2.03, −2.36	−4.47	−2.87	1.60	1.91	
HZ-TIPS[7e]	634	60000	0.17, 0.69	−1.48, −1.86	−4.87	−3.41	1.46	1.82	
OZ-Mes[7p]	649, 692, 757	87000	0.09, 0.30	−1.82	−4.44	−3.09	1.35	1.56	−3.8
OZ-TIPS[7e]	668, 719, 795	83300	0.02, 0.22, 0.61	−1.30, −1.56, −1.82	−4.73	−3.60	1.13	1.50	−3.9
HR-NZ	672, 800, 895	79600	0.08,0.26	−1.46, −1.82	−4.73	−3.42	1.31	1.33	−5.2
JA-NA[10h]	880, 1014		0.35	−0.96, −1.18	−5.10	−3.91	1.19	1.20	

[a]HOMO = −(4.8 + E_{ox}^{onset}) eV, LUMO = −(4.8 + E_{red}^{onset}) eV, where E_{ox}^{onset} and E_{red}^{onset} are the onset potential of the first oxidation and reduction wave, respectively, vs Fc/Fc$^+$ couple. E_g^{EC} = HOMO − LUMO. E_g^{opt} is the optical energy gap obtained from the lowest energy absorption onset. ΔE_{S-T}^{Exp} is experimentally measured singlet−triplet energy gap by SQUID method.

DOI: 10.1021/jacs.6b06188
J. Am. Chem. Soc. 2016, 138, 10323−10330

carbon−carbon triple bonds. Therefore, although **OZ-TIPS** is shorter than **HR-NZ** in the zethrene skeleton, it actually showed smaller singlet−singlet and singlet−triplet energy gaps. In addition, the existence of two electron-donating alkoxy groups in **OZ-Mes** leads to a smaller singlet−triplet gap compared to that of **HR-NZ**. These results indicate how substituents can have an important impact on the energy gaps and diradical characters of organic open-shell singlet diradicaloid systems.

Theoretical Calculations and Discussion. To understand in detail the diradical nature of the singlet ground state of **HR-NZ** in comparison to that of **JA-NA** and the parent higher order acenes and zethrenes, we conducted electronic structure calculations at the restricted active space spin-flip (RAS-SF)[13a] level of theory, which has been shown to properly deal with strongly correlated electrons in systems with important diradical (or polyradical) character and provide reliable results measuring the molecular radical character and excitation energies.[13b] The diradical character degree of the ground state singlet was estimated from the electron occupancies of the frontier natural orbitals through the Yamaguchi's scheme (y_0)[14] and by the number of unpaired electrons (N_U) according to eq 1,[15] where $\{n_i\}$ are the natural occupation numbers from the one-particle density matrix.

$$N_U = \sum_i (1 - \mathrm{abs}(1 - n_i)) \quad (1)$$

The computed values for N_U, y_0, and singlet−triplet energy difference (ΔE_{S-T}) are summarized in Table 2. Our calculations

Table 2. Calculated Diradical Character (y_0), Number of Unpaired Electrons (N_U), and Singlet−Triplet Energy Gaps (ΔE_{S-T}, kcal/mol) at the RAS-SF/6-31G(d,p) Level[a]

mol.	y_0	N_u	ΔE_{S-T}	mol.	y_0	N_u	ΔE_{S-T}
Zth	0.00	0.28	−37.8	**HexA**	0.04	0.61	−17.0
HZ	0.04	0.57	−18.3	**HepA**	0.08	0.79	−11.3
OZ	0.13	0.92	−9.2	**OA**	0.15	1.02	−7.5
NZ	0.25	1.21	−5.2	**NA**	0.22	1.15	−5.7
HR-NZ	0.25	1.20	−5.4	**JA-NA**	0.20	1.15	−5.8

[a]HexA: hexacene, HepA: heptacene, OA: octacene, NA: nonacene.

predict that the parent zethrene has a zero diradical character with a closed-shell ground state, which is in accordance with experimental observations.[7i] The extended zethrenes, all have an open-shell singlet ground state and with extension of the molecule length, the diradical character increases while the singlet−triplet energy gap decreases (Table 2). We theoretically found that **HR-NZ** possesses a moderate diradical character (y_0 = 0.25 and N_U = 1.20) in singlet ground state with a small ΔE_{S-T} value (−5.4 kcal/mol), in very good agreement with the experimental gap and very close to the results for the parent nonazethrene (y_0 = 0.25, N_U = 1.21 and ΔE_{S-T} = −5.2 kcal/mol). Higher order acenes (hexacene to nonacene) are found to have open-shell singlet ground state and, similar to zethrene series, the diradical character becomes larger with the increase of the number of benzenoid rings.

Interestingly, although the ΔE_{S-T} energy gap of zethrene is much larger than that in hexacene, the decrease of the gap with the molecular size is clearly much faster within the zethrene series, and at 8−9 rings, the computed values are very close to each other (Figure 6). This trend is also recovered by density functional theory (DFT)-based methods (Tables S1 and S2).

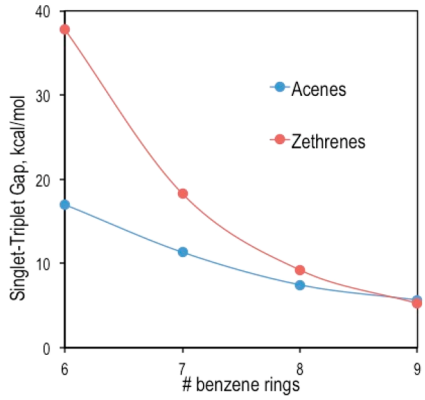

Figure 6. Singlet−triplet energy gap (in kcal/mol) for the acene and zenthrene series computed at the RAS-SF/6-31G(d,p) level.

The origin of the different behavior between acene and zethrene series requires deeper investigation (*vide infra*).

Frontier natural orbitals responsible of the diradical character of the **JA-NA** and **HR-NZ** molecules are shown in Figure 7. It is noteworthy that the unpaired electrons in **JA-NA** are localized at the center of the molecule, whereas in **HR-NZ**, they are at the edges.

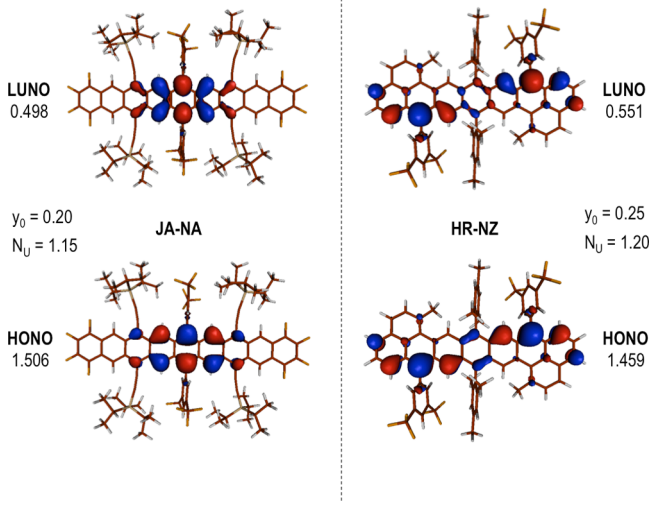

Figure 7. HONO, LUNO, and electron occupancies and diradical character indicators y_0 and N_U for **JA-NA** and **HR-NZ** molecules computed at the RAS-SF/6-31G(d,p) level.

To explore the nature of diradical character in acenes and zethrenes, we have decomposed the computed wave functions in different contributions by using fragment orbitals. From such localized orbitals, it is possible to express the wave function of the ground state singlet as the interaction of two radical centers (A and B). In other words, as a combination of neutral contributions (NE, 1 electron on each center) and charge resonances (CR, 2 electrons on 1 center), as indicated in eq 2

$$|\Psi_{S=0}\rangle = c_{NE}|\Psi_{NE}\rangle + c_{CR}|\Psi_{CR}\rangle \quad (2)$$

where NE and CR terms can be explicitly expressed as

$$|\Psi_{NE}\rangle = |A(\alpha)B(\beta)\rangle + |A(\beta)B(\alpha)\rangle \quad (3)$$

DOI: 10.1021/jacs.6b06188
J. Am. Chem. Soc. 2016, 138, 10323−10330

$$|\Psi_{CR}\rangle = |A(\alpha)A(\beta)\rangle + |B(\alpha)B(\beta)\rangle \quad (4)$$

Evidently, the triplet state only contains NE terms (2 unpaired electrons).

$$|\Psi_{S=1}\rangle = |A(\alpha)B(\alpha)\rangle \quad (5)$$

From this scheme, the c_{CR} amplitudes correspond to charge resonances between the two radical centers and can be used as a measure of their interaction. The frontier localized molecular orbitals of some acene and zethrene molecules are shown in Figure 8, and the amounts of CR (in %) in the ground state

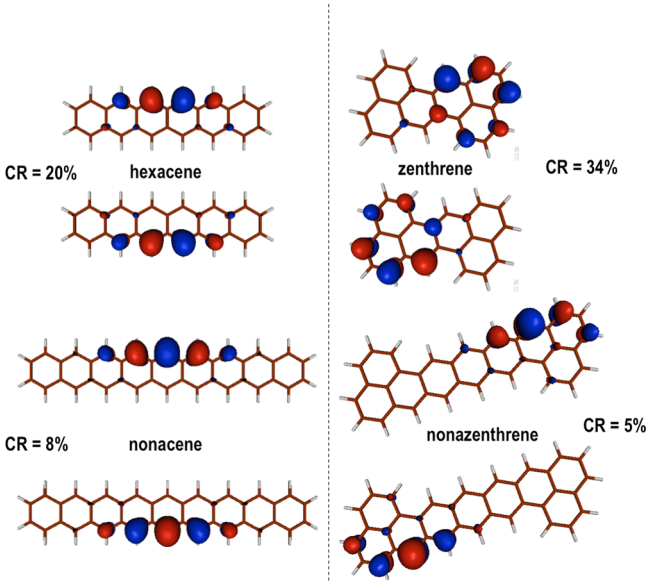

Figure 8. Frontier localized molecular orbitals of hexacene, nonacene, zethrene, and nonazethrene.

singlet along the acene and zenthrene series are presented in Figure 9. The CR contribution in zethrene is much larger than

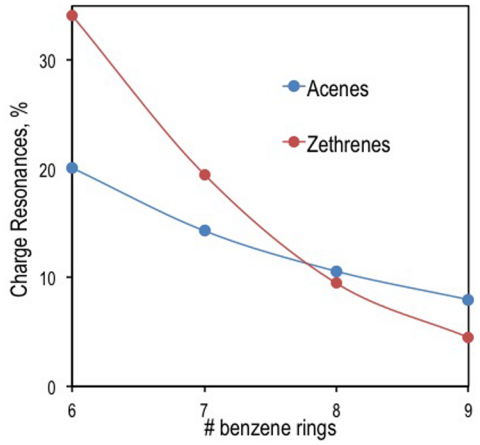

Figure 9. Charge resonance contributions (in %) along the acene and zethrene series computed at the RAS-SF/6-31G(d,p) level.

that in hexacene, indicating stronger interaction between radicals. This contribution decreases with the number of benzenoid rings, but this decrease is faster within the zethrene series. CR contributions in nonacene are larger than that in nonazethrene, suggesting larger diradical character in the latter.

In the same sense, analysis of the spin densities obtained at the DFT level also indicates significant differences between acenes and zethrenes (Figures 10 and S1). For example, the

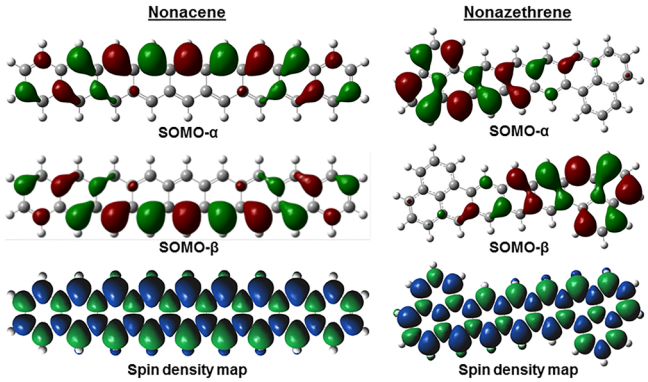

Figure 10. Calculated SOMO-α/-β profiles and spin density maps of the singlet diradicals of parent nonacene (left) and nonazethrene (right).

singly occupied molecular orbital (SOMO) profiles of the α and β spins of the nonacene are mainly delocalized along the two zigzag edges with a disjointed character, and the spins are thus mainly distributed along the two zigzag edges with the central carbons having the highest spin density. However, for nonazethrene, the α and β spins are mainly delocalized at the two terminal phenalenyl moieties with a similar disjoint character, and the spins are distributed through the whole π-conjugated framework with the zigzag edges having higher spin density. Such a difference on SOMO profiles and spin distribution resembles the picture obtained by CR analysis performed above and suggests that one needs to strategically put stabilizing groups to the zigzag edges of acenes and the phenalenyl moieties of zethrenes. Indeed, both **JA-NA** and **HR-NZ** are appropriately designed; thus, relatively stable materials are obtained for full characterizations. Calculations on the substituted nonacene **JA-NA** and nonazethrene **HR-NZ** reveal similar SOMO profiles and spin distribution, with slightly different diradical characters and singlet−triplet energy gaps (Table S1 and Figure S1).

Overall, these results point toward the different localization of the unpaired electrons as the origin for the different behavior of the acene and zethrene series, that is, the faster decrease of singlet−triplet gap and faster increase of radical character in zethrenes can be understood to be due to a faster decrease of the interaction between the radical centers. Calculations also show that **JA-NA** has a slightly larger singlet−triplet energy difference (5.8 kcal/mol) than **HR-NZ** (5.4 kcal/mol), indicating that it may require even higher temperature to thermally populate the singlet species to the paramagnetic triplet species and result in significant ESR/SQUID signal.

CONCLUSIONS

The first substituted nonazethrene **HR-NZ** was synthesized and fully characterized. It shows an open-shell singlet ground state with a moderate diradical character and a small singlet−triplet energy gap (ΔE_{S-T} = −5.2 kcal/mol based on SQUID data). Consequently, **HR-NZ** exhibited NMR broadening and paramagnetic activity at room temperature. It has a small energy gap and displays amphoteric redox behavior, allowing us to access their stable radical cation and dication species. A

DOI: 10.1021/jacs.6b06188
J. Am. Chem. Soc. 2016, 138, 10323−10330

comparison between our **HR-NZ** and Anthony's **JA-NA** and more generally between the extended zethrenes and higher order acenes reveals a faster decrease of singlet−triplet energy gap and a faster increase of radical character with the increase of number of benzenoid rings in zethrene series. Such a significant difference can be explained by the different localization of the unpaired electrons and the different charge resonance contribution in the acene and zethrene series. Our studies indicate that spatial localization of the frontier molecular orbitals play a very important role on the nature of radical character as well as the excitation energy, and this must be considered in the design of open-shell singlet diradicaloids and polyradicaloids in the future.

■ ASSOCIATED CONTENT

Supporting Information

The Supporting Information is available free of charge on the ACS Publications website at DOI: 10.1021/jacs.6b06188.

Synthetic procedures and characterization data of all other new compounds; ^{1}H−^{1}H COSY NMR of **HR-NZ**; details for all physical characterizations and theoretical calculations (PDF)

■ AUTHOR INFORMATION

Corresponding Authors

*chmwuj@nus.edu.sg

*david.casanova@ehu.eus

Notes

The authors declare no competing financial interest.

■ ACKNOWLEDGMENTS

This work was financially supported by the MOE Tier 3 Programme (MOE2014-T3-1-004), Tier 2 grant (MOE2014-T2-1-080), and A*STAR JCO grant (1431AFG100). R.H. acknowledges the scholarship support from the Chinese Scholarship Council ([2014]3026). D.C. acknowledges the Basque Government (project IT588-13) for financial support and SGIker for allocation of computational resources.

■ REFERENCES

(1) Recent review articles: (a) Sun, Z.; Ye, Q.; Chi, C.; Wu, J. *Chem. Soc. Rev.* **2012**, *41*, 7857. (b) Shimizu, A.; Hirao, Y.; Kubo, T.; Nakano, M.; Botek, E.; Champagne, B. *AIP Conf. Proc.* **2009**, *1504*, 399. (c) Sun, Z.; Zeng, Z.; Wu, J. *Chem. - Asian J.* **2013**, *8*, 2894. (d) Abe, M. *Chem. Rev.* **2013**, *113*, 7011. (e) Sun, Z.; Zeng, Z.; Wu, J. *Acc. Chem. Res.* **2014**, *47*, 2582. (f) Kubo, T. *Chem. Rec.* **2015**, *15*, 218. (g) Zeng, Z.; Shi, X.; Chi, C.; López Navarrete, J. T.; Casado, J.; Wu, J. *Chem. Soc. Rev.* **2015**, *44*, 6578.

(2) Examples of bisphenalenyls: (a) Ohashi, K.; Kubo, T.; Masui, T.; Yamamoto, K.; Nakasuji, K.; Takui, T.; Kai, Y.; Murata, I. *J. Am. Chem. Soc.* **1998**, *120*, 2018. (b) Kubo, T.; Sakamoto, M.; Akabane, M.; Fujiwara, Y.; Yamamoto, K.; Akita, M.; Inoue, K.; Takui, T.; Nakasuji, K. *Angew. Chem., Int. Ed.* **2004**, *43*, 6474. (c) Kubo, T.; Shimizu, A.; Sakamoto, M.; Uruichi, M.; Yakushi, K.; Nakano, M.; Shiomi, D.; Sato, K.; Takui, T.; Morita, Y.; Nakasuji, K. *Angew. Chem., Int. Ed.* **2005**, *44*, 6564. (d) Shimizu, A.; Uruichi, M.; Yakushi, K.; Matsuzaki, H.; Okamoto, H.; Nakano, M.; Hirao, Y.; Matsumoto, K.; Kurata, H.; Kubo, T. *Angew. Chem., Int. Ed.* **2009**, *48*, 5482. (e) Shimizu, A.; Kubo, T.; Uruichi, M.; Yakushi, K.; Nakano, M.; Shiomi, D.; Sato, K.; Takui, T.; Hirao, Y.; Matsumoto, K.; Kurata, H.; Morita, Y.; Nakasuji, K. *J. Am. Chem. Soc.* **2010**, *132*, 14421. (f) Shimizu, A.; Hirao, Y.; Matsumoto, K.; Kurata, H.; Kubo, T.; Uruichi, M.; Yakushi, K. *Chem. Commun.* **2012**, *48*, 5629.

(3) Examples of anthenes and periacenes: (a) Konishi, A.; Hirao, H.; Nakano, M.; Shimizu, A.; Botek, E.; Champagne, B.; Shiomi, D.; Sato, K.; Takui, T.; Matsumoto, K.; Kurata, H.; Kubo, T. *J. Am. Chem. Soc.* **2010**, *132*, 11021. (b) Konishi, A.; Hirao, Y.; Matsumoto, K.; Kurata, H.; Kishi, R.; Shigeta, Y.; Nakano, M.; Tokunaga, K.; Kamada, K.; Kubo, T. *J. Am. Chem. Soc.* **2013**, *135*, 1430. (c) Liu, J.; Ravat, P.; Wagner, M.; Baumgarten, M.; Feng, X.; Müllen, K. *Angew. Chem., Int. Ed.* **2015**, *54*, 12442.

(4) Example of indenofluorenes: (a) Chase, D. T.; Rose, B. D.; McClintock, S. P.; Zakharov, L. N.; Haley, M. M. *Angew. Chem., Int. Ed.* **2011**, *50*, 1127. (b) Shimizu, A.; Tobe, Y. *Angew. Chem., Int. Ed.* **2011**, *50*, 6906. (c) Fix, A. G.; Deal, P. E.; Vonnegut, C. L.; Rose, B. D.; Zakharov, L. N.; Haley, M. M. *Org. Lett.* **2013**, *15*, 1362. (d) Rose, B. D.; Vonnegut, C. L.; Zakharov, L. N.; Haley, M. M. *Org. Lett.* **2012**, *14*, 2426. (e) Shimizu, A.; Kishi, R.; Nakano, M.; Shiomi, D.; Sato, K.; Takui, T.; Hisaki, I.; Miyata, M.; Tobe, Y. *Angew. Chem., Int. Ed.* **2013**, *52*, 6076. (f) Fix, A. G.; Chase, D. T.; Haley, M. M. *Top. Curr. Chem.* **2012**, *349*, 159. (g) Miyoshi, H.; Nobusue, S.; Shimizu, A.; Hisaki, I.; Miyata, M.; Tobe, Y. *Chem. Sci.* **2014**, *5*, 163. (h) Young, B. S.; Chase, D. T.; Marshall, J. L.; Vonnegut, C. L.; Zakharov, L. N.; Haley, M. M. *Chem. Sci.* **2014**, *5*, 1008. (i) Luo, D.; Lee, S.; Zheng, B.; Sun, Z.; Zeng, W.; Huang, K.-W.; Furukawa, K.; Kim, D.; Webster, R. D.; Wu, J. *Chem. Sci.* **2014**, *5*, 4944.

(5) Examples of extended *p*-quinodimethanes: (a) Zhu, X.; Tsuji, H.; Nakabayashi, H.; Ohkoshi, S.; Nakamura, E. *J. Am. Chem. Soc.* **2011**, *133*, 16342. (b) Zeng, Z.; Sung, Y. M.; Bao, N.; Tan, D.; Lee, R.; Zafra, J. L.; Lee, B. S.; Ishida, M.; Ding, J.; López Navarrete, J. T.; Li, Y.; Zeng, W.; Kim, D.; Huang, K.-W.; Webster, R. D.; Casado, J.; Wu, J. *J. Am. Chem. Soc.* **2012**, *134*, 14513. (c) Zeng, Z.; Ishida, M.; Zafra, J. L.; Zhu, X.; Sung, Y. M.; Bao, N.; Webster, R. D.; Lee, B. S.; Li, R.-W.; Zeng, W.; Li, Y.; Chi, C.; López Navarrete, J. T.; Ding, J.; Casado, J.; Kim, D.; Wu, J. *J. Am. Chem. Soc.* **2013**, *135*, 6363. (d) Zeng, Z.; Lee, S.; Zafra, J. L.; Ishida, M.; Zhu, X.; Sun, Z.; Ni, Y.; Webster, R. D.; Li, R.-W.; López Navarrete, J. T.; Chi, C.; Ding, J.; Casado, J.; Kim, D.; Wu, J. *Angew. Chem., Int. Ed.* **2013**, *52*, 8561. (e) Zeng, Z.; Lee, S.; Zafra, J. L.; Ishida, M.; Bao, N.; Webster, R. D.; López Navarrete, J. T.; Ding, J.; Casado, J.; Kim, D.; Wu, J. *Chem. Sci.* **2014**, *5*, 3072. (f) Zeng, Z.; Wu, J. *Chem. Rec.* **2015**, *15*, 322. (g) Zeng, Z.; Lee, S.; Son, M.; Fukuda, K.; Burrezo, P. M.; Zhu, X.; Qi, Q.; Li, R.-W.; López Navarrete, J. T.; Ding, J.; Casado, J.; Nakano, M.; Kim, D.; Wu, J. *J. Am. Chem. Soc.* **2015**, *137*, 8572. (h) Lim, Z. L.; Zheng, B.; Huang, K.-W.; Liu, Y.; Wu, J. *Chem. - Eur. J.* **2015**, *21*, 18724.

(6) Review articles on higher order acenes: (a) Bendikov, M.; Wudl, F.; Perepichka, D. F. *Chem. Rev.* **2004**, *104*, 4891. (b) Anthony, J. E. *Chem. Rev.* **2006**, *106*, 5028. (c) Anthony, J. E. *Angew. Chem., Int. Ed.* **2008**, *47*, 452. (d) Ye, Q.; Chi, C. *Chem. Mater.* **2014**, *26*, 4046. (e) Bettinger, H. F.; Tönshoff, C. *Chem. Rec.* **2015**, *15*, 364.

(7) (a) Umeda, R.; Hibi, D.; Miki, K.; Tobe, Y. *Org. Lett.* **2009**, *11*, 4104. (b) Wu, T. C.; Chen, C. H.; Hibi, D.; Shimizu, A.; Tobe, Y.; Wu, Y. T. *Angew. Chem., Int. Ed.* **2010**, *49*, 7059. (c) Sun, Z.; Huang, K.-W.; Wu, J. *Org. Lett.* **2010**, *12*, 4690. (d) Sun, Z.; Huang, K.-W.; Wu, J. *J. Am. Chem. Soc.* **2011**, *133*, 11896. (e) Li, Y.; Heng, W.-K.; Lee, B. S.; Aratani, N.; Zafra, J. L.; Bao, N.; Lee, R.; Sung, Y. M.; Sun, Z.; Huang, K.-W.; Webster, R. D.; López Navarrete, J. T.; Kim, D.; Osuka, A.; Casado, J.; Ding, J.; Wu, J. *J. Am. Chem. Soc.* **2012**, *134*, 14913. (f) Sun, Z.; Lee, S.; Park, K.; Zhu, X.; Zhang, W.; Zheng, B.; Hu, P.; Zeng, Z.; Das, S.; Li, Y.; Chi, C.; Li, R.; Huang, K.-W.; Ding, J.; Kim, D.; Wu, J. *J. Am. Chem. Soc.* **2013**, *135*, 18229. (g) Sun, Z.; Wu, J. *J. Org. Chem.* **2013**, *78*, 9032. (h) Shan, L.; Liang, Z.-X.; Xu, X.-M.; Tang, Q.; Miao, Q. *Chem. Sci.* **2013**, *4*, 3294. (i) Zafra, J. L.; González Cano, R. C.; Ruiz Delgado, M. C.; Sun, Z.; Li, Y.; López Navarrete, J. T.; Wu, J.; Casado, J. *J. Chem. Phys.* **2014**, *140*, 054706. (j) Li, Y.; Huang, K.-W.; Sun, Z.; Webster, R. D.; Zeng, Z.; Zeng, W.; Chi, C.; Furukawa, K.; Wu, J. *Chem. Sci.* **2014**, *5*, 1908. (k) Das, S.; Lee, S.; Son, M.; Zhu, X.; Zhang, W.; Zheng, B.; Hu, P.; Zeng, Z.; Sun, Z.; Zeng, W.; Li, R. W.; Huang, K.-W.; Ding, J.; Kim, D.; Wu, J. *Chem. - Eur. J.* **2014**, *20*, 11410. (l) Sun, Z.; Zheng, B.; Hu, P.; Huang, K.-W.; Wu, J. *ChemPlusChem* **2014**, *79*, 1549. (m) Hsieh, Y.-C.; Fang, H.-Y.; Chen, Y.-T.; Yang, R.; Yang, C.-I.; Chou, P.-T.; Kuo, M.-Y.; Wu, Y.-T. *Angew. Chem., Int. Ed.*

2015, *54*, 3069. (n) Hu, P.; Lee, S.; Herng, T. S.; Aratani, N.; Gonçalves, T. P.; Qi, Q.; Shi, X.; Yamada, H.; Huang, K.-W.; Ding, J.; Kim, D.; Wu, J. *J. Am. Chem. Soc.* **2016**, *138*, 1065. (o) Hu, P.; Lee, S.; Park, K. H.; Das, S.; Herng, T. S.; Gonçalves, T. P.; Huang, K.-W.; Ding, J.; Kim, D.; Wu, J. *J. Org. Chem.* **2016**, *81*, 2911. (p) Yadav, P.; Das, S.; Phan, H.; Herng, T. S.; Ding, J.; Wu, J. *Org. Lett.* **2016**, *18*, 2886. (q) Zeng, W.; Sun, Z.; Herng, T. S.; Gonçalves, T. P.; Gopalakrishna, T. Y.; Huang, K.-W.; Ding, J.; Wu, J. *Angew. Chem., Int. Ed.* **2016**, *55*, 8615.

(8) Bendikov, M.; Duong, H. M.; Starkey, K.; Houk, K. N.; Carter, E. A.; Wudl, F. *J. Am. Chem. Soc.* **2004**, *126*, 7416.

(9) (a) dos Santos, M. C. *Phys. Rev. B: Condens. Matter Mater. Phys.* **2006**, *74*, 045426. (b) Hachmann, J.; Dorando, J. J.; Avilés, M.; Chan, G. K.-L. *J. Chem. Phys.* **2007**, *127*, 134309. (c) Jiang, D.; Dai, S. *J. Phys. Chem. A* **2008**, *112*, 332.

(10) (a) Payne, M. M.; Parkin, S. R.; Anthony, J. E. *J. Am. Chem. Soc.* **2005**, *127*, 8028. (b) Chun, D.; Cheng, Y.; Wudl, F. *Angew. Chem., Int. Ed.* **2008**, *47*, 8380. (c) Kaur, I.; Stein, N. N.; Kopreski, R. P.; Miller, G. P. *J. Am. Chem. Soc.* **2009**, *131*, 3424. (d) Mondal, R.; Tönshoff, C.; Khon, D.; Neckers, D. C.; Bettinger, H. F. *J. Am. Chem. Soc.* **2009**, *131*, 14281. (e) Tönshoff, C.; Bettinger, H. F. *Angew. Chem., Int. Ed.* **2010**, *49*, 4125. (f) Qu, H.; Chi, C. *Org. Lett.* **2010**, *12*, 3360. (g) Kaur, I.; Jazdzyk, M.; Stein, N. N.; Prusevich, P.; Miller, G. P. *J. Am. Chem. Soc.* **2010**, *132*, 1261. (h) Purushothaman, B.; Bruzek, M.; Parkin, S. R.; Miller, A. F.; Anthony, J. E. *Angew. Chem., Int. Ed.* **2011**, *50*, 7013. (i) Watanabe, M.; Chang, Y. J.; Liu, S. W.; Chao, T. H.; Goto, K.; Islam, M. M.; Yuan, C. H.; Tao, Y. T.; Shinmyozu, T.; Chow, T. J. *Nat. Chem.* **2012**, *4*, 574.

(11) Bleaney, B.; Bowers, K. D. *Proc. R. Soc. London, Ser. A* **1952**, *214*, 451.

(12) Di Motta, S.; Negri, F.; Fazzi, D.; Castiglioni, C.; Canesi, E. V. *J. Phys. Chem. Lett.* **2010**, *1*, 3334.

(13) (a) Casanova, D.; Head-Gordon, M. *Phys. Chem. Chem. Phys.* **2009**, *11*, 9779. (b) Das, S.; Herng, T. S.; Zafra, J. L.; Burrezo, P. M.; Kitano, M.; Ishida, M.; Gopalakrishna, Y. T.; Hu, P.; Osuka, A.; Casado, J.; Ding, J.; Casanova, D.; Wu, J. *J. Am. Chem. Soc.* **2016**, *138*, 7782.

(14) Minami, T.; Nakano, M. *J. Phys. Chem. Lett.* **2012**, *3*, 145.

(15) Head-Gordon, M. *Chem. Phys. Lett.* **2003**, *372*, 508.

DOI: 10.1021/jacs.6b06188
J. Am. Chem. Soc. 2016, 138, 10323−10330